Estimation of Optical Turbulence Using Multiscale Atmospheric Models

Yao Wang and Sukanta Basu

Department of Marine, Earth, & Atmospheric Sciences, North Carolina State University, Raleigh, NC, USA

Introduction

Optical Turbulence (O.T.)

- The wave phase and amplitude of the optical and electromagnetic waves are highly affected by the small-scale variation of temperature and specific humidity.
- The turbulent atmosphere causes the intensity of a light beam to fluctuate or scintillate, causes beam to wander, and causes the distortion and random displacement of images. (Hutt, 1999)

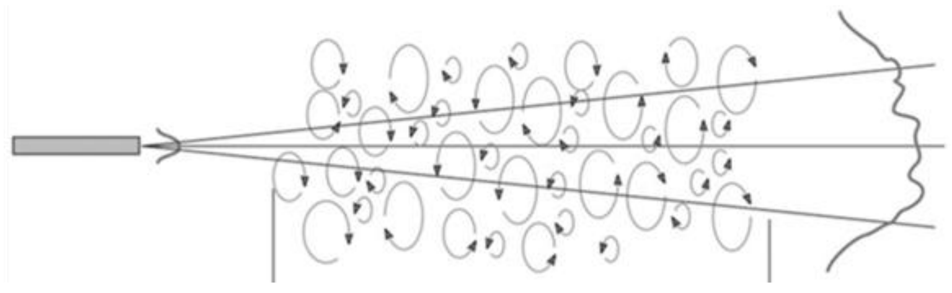

Fig. 1 A laser beam propagating through the atmosphere spreads due to diffraction but is also influenced by turbulence in the form of randomly varying eddies. (Burger et al., 2008)

Fig. 2 Double star Zeta Aquarii (which has a separation of 2 arcseconds) is blurred by atmospheric turbulence. (Image Courtesy: *Alan Adler)*

Applications

- Estimation and prediction of optical turbulence are significant to a wide range of applications: environmental monitoring, optical communication, astronomy, sensing with detection, reconnaissance and identification, guiding systems or directed-energy systems. (See Cheinet et al., 2010 and the references therein)

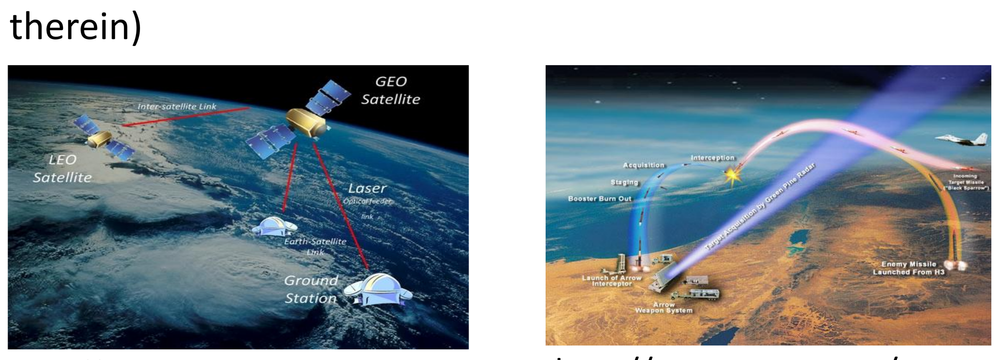

http://spacelaser.weebly.com http://nextbigfuture.com/

Fig 3 Laser communication (left) and guiding systems (right).

Refractive index structure parameter

- Under some approximations, the optical turbulence effects can be quantified in terms of structure parameter (C_n^2) of refractive index (n) (units $m^{-2/3}$). (Tatarski 1961)

$$C_n^2 = \langle [n(\tilde{r}_1) - n(\tilde{r}_2)]^2 \rangle / |\tilde{r}_1 - \tilde{r}_2|^{2/3}$$

Estimation C_n^2 using meteorological models

- The small-scale turbulence is primarily driven by the meteorological forcings including synoptic-scale variability, diurnal cycles, large-scale gravity waves, convective plumes, and mesoscale circulations etc.
- C_n^2 is chosen to describe the effect of the optical turbulence. It depends on temperature structure parameter C_T^2, if the minor wavelength and humidity dependence are ignored.
- Numerical meteorological models can be utilized to estimate C_T^2 from temperature and turbulent variables.

$$C_n^2 = (79PT^{-2} \times 10^{-6})^2 C_T^2$$

Indirect C_T^2 and C_n^2 Calculations

- **Monin-Obukhov similarity functions**

$$\frac{C_T^{\,2} z^{2/3}}{\theta_*^2} = f_T(\zeta)$$

ζ Stability parameter (z/L)

θ_* Generic turbulent temperature scale

Stably Stratified Surface Layer

MOST 1. Wyngaard-Coté-Andreas (1989)

$$f_T(\zeta) = c_{T1}\left[1 + c_{T2}\zeta^{2/3}\right]$$

MOST 2. Thiermann-Grassl (1992)

$$f_T(\zeta) = 6.34\left[1 + 7\zeta + 20\zeta^2\right]^{1/3}$$

MOST 3. Kink (Hartogensis, 2006)

$$f_T = \begin{cases} 5.5 & \text{for } \zeta < 0.1 \\ 5.5(\zeta/0.1)^{2/5} & \text{otherwise} \end{cases}$$

- **Regression model function**

Sadot et al. (1992)

$$C_n^2 = a_1 W + b_1 T + c_1 RH + c_2 RH^2 + c_3 RH^3 + d_1 WS + d_2 WS^2 + d_3 WS^3 + e$$

W is temporal hour weight; **T** is temperature; **RH** is relative humidity
a, b, c, d and **e** are numerical regression coefficients.

Case Study: CASES-99

October 23-25, 1999

The first night was intermittently turbulent, with several turbulent mixing events (Sun et al. 2003a). A low-level jet (LLJ) event occurred with a mean wind speed of 7.6 m s^{-1}. The Height of the LLJ was approximately 100 m.

In the second (turbulent) night, a continuous LLJ with mean wind speed of 15.2 m s^{-1} was observed. The LLJ height was approximately 200 m and it increased throughout the night.

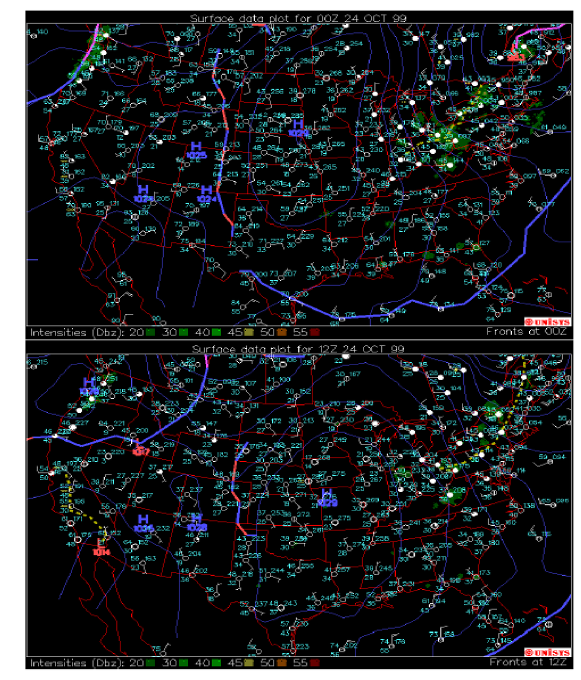

Fig. 4 Surface analysis at 0 UTC (top) and 12 UTC (bottom) on October 24, 1999. The Midwest of the U.S. was dominated by a synoptic-scale surface high pressure system.

Observations

A diverse suite of observational datasets were utilized for model validation. These datasets were collected by a Doppler lidar, a small-aperture scintillometer, sonic anemometers, and a sounding system etc.

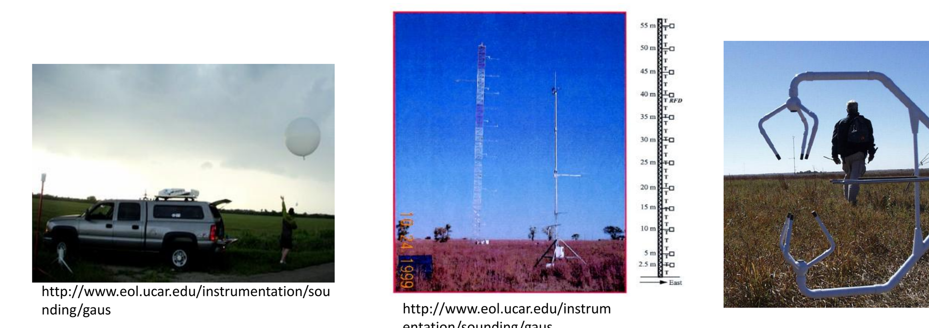

http://www.eol.ucar.edu/instrumentation/sounding/gaus http://www.eol.ucar.edu/instrumentation/sounding/gaus

Fig. 5 Pictures of observation instruments: sounding (left), tower (middle), and sonic anemometer (right).

Numerical-modeling Framework

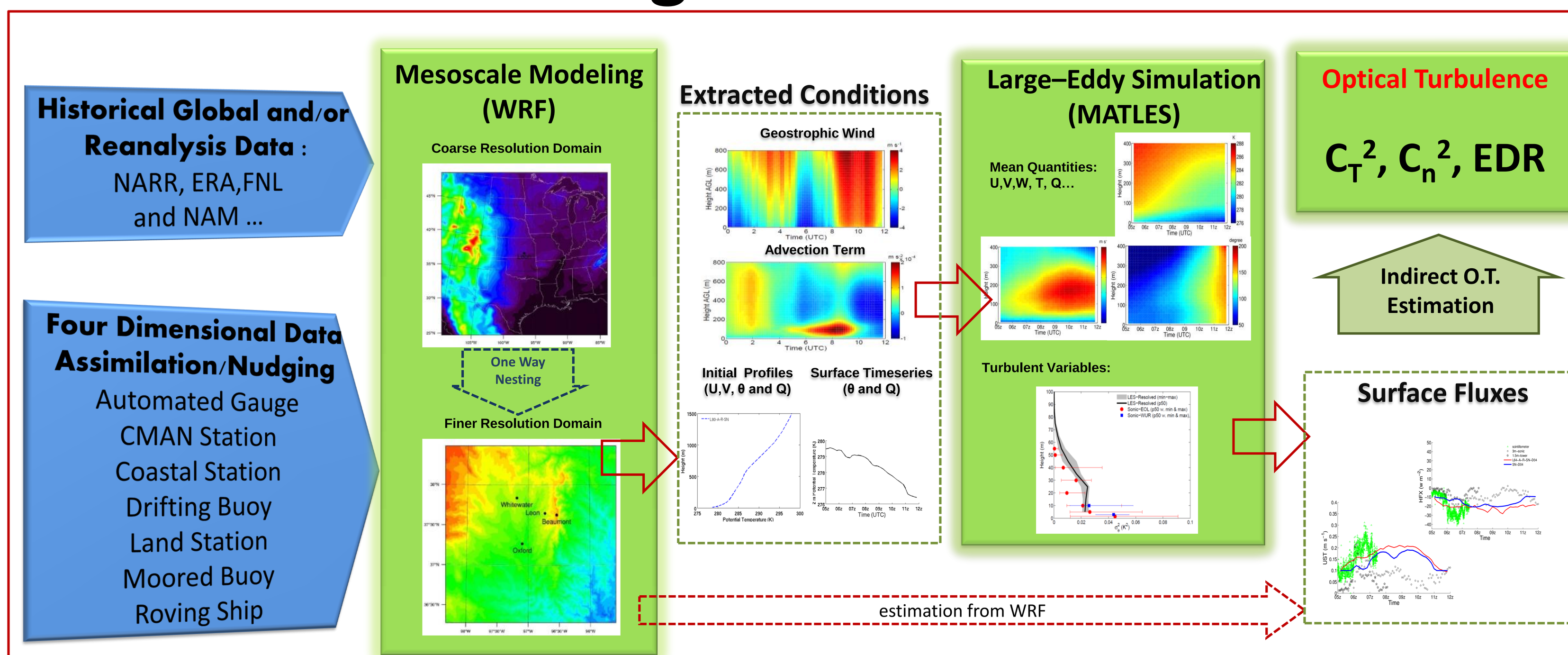

- Observational datasets were assimilated into the WRF model.
- From the WRF model, the Initial conditions, time-dependent lower-boundary conditions (e.g., near-surface air temperature), and time-height-dependent large-scale forcings (e.g., geostrophic wind, mesoscale advection of temperature) were extracted for LES runs
- The tuning-free SGS model, locally-averaged scale-dependent dynamic (LASDD) subgrid-scale (SGS) model was applied in Large-eddy simulation.

Model Configuration

WRF

Model:	WRF v3.3	**Data Assimilation:**	
Initial condition:	NARR	U, V, and T: NCEP ADP Global Surface Observational Weather Data	
Grid size:	27/9/3/1 km		
PBL scheme:	YSU (bug-fixed version)	obs_coef	= 6.E-4 s^{-1}, (1/30 min)
Ra_scheme:	RRTMG	obs_rinxy	= 270/90/30/10 km
MP_scheme:	WSM 5-class	obs_rinsig	= 0.002 (eta)
CP_scheme:	Kain-Fritsch (d1 and d2)	obs_twindo	= 10 min -> means +/- 10 min around observation

LES

Domain size: 800 m × 800 m × 790 m Time: 05z-12z Oct. 24th Grid size: 10 m

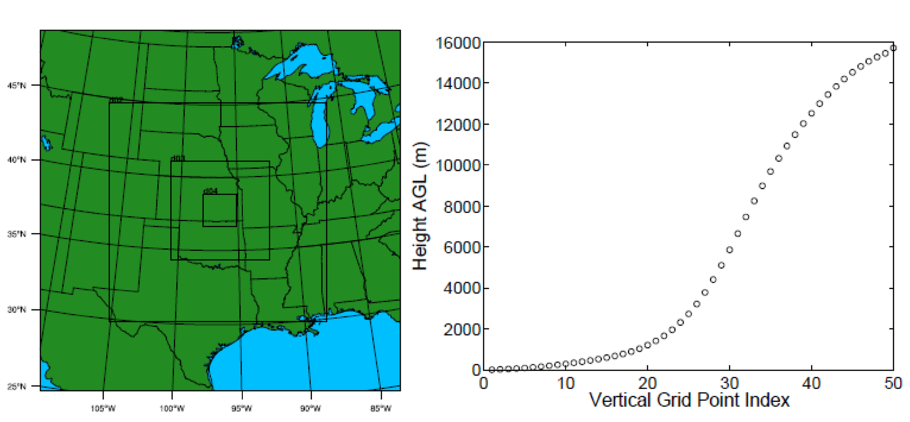

Fig. 6 The WRF model nested domains (left), and locations of vertical grid points (right).

Results

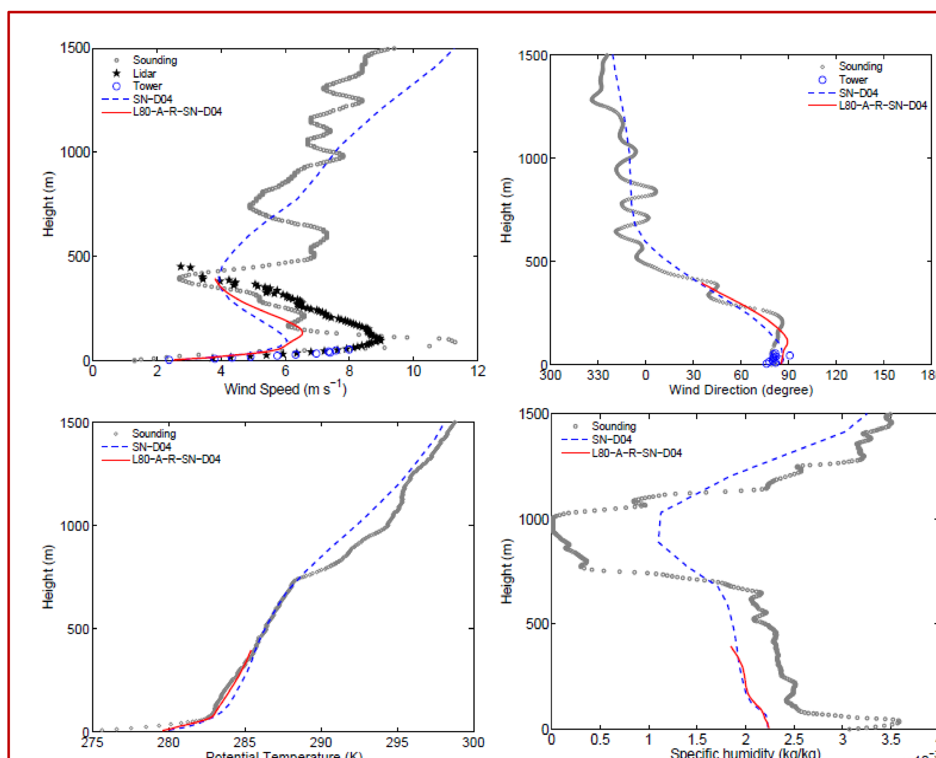

Fig. 7 Plots of the wind speed (upper left), wind direction (upper right), potential temperature (lower left), and specific humidity (lower right) profiles at 7 UTC.

- The WRF model simulated a weaker and slightly higher LLJ due to the enhanced diffusion.
- The modeled LLJs were 3 hours delayed comparing with the observed.
- The LES model simulated a stronger jet and slightly jet higher due to lack of subsidence.
- WRF and LES captured the wind direction and potential temperature profiles remarkably well.
- WRF and LES did not show the intermittency in surface fluxes during nighttime.

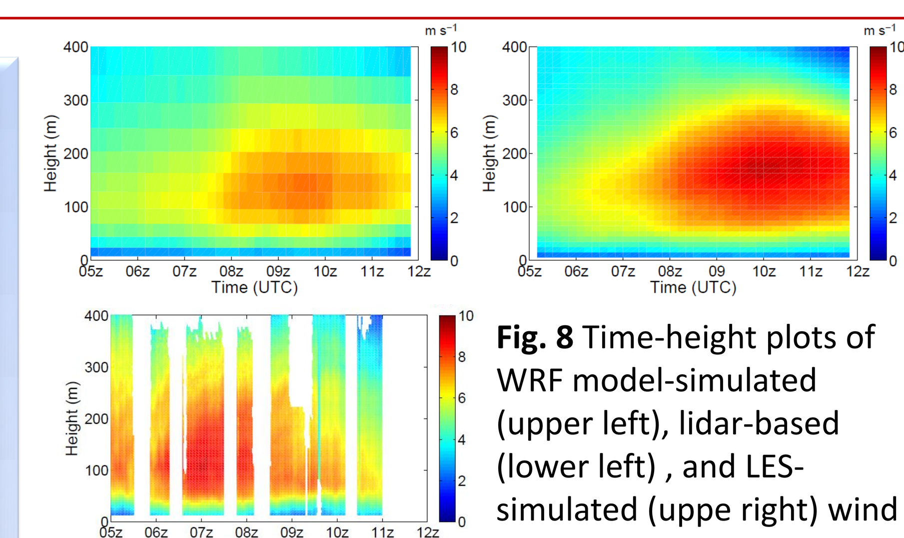

Fig. 8 Time-height plots of WRF model-simulated (upper left), lidar-based (lower left) , and LES-simulated (uppe right) wind speeds.

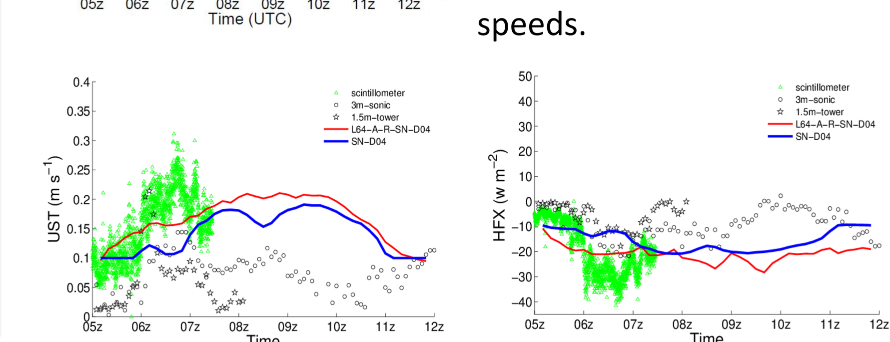

Fig. 9 Time series of surface friction velocity (left) and sensible heat flux (right) .

- Diurnal cycle of C_n^2 were captured reasonably by the WRF Model.
- C_n^2 was underestimated during the intermittently turbulent night by both WRF and LES.
- MOST function 2 (Wyngaard-Coté-Andreas) estimated C_n^2 relatively better during the daytime. All MOST functions showed the limitation of calculating O.T. during the nighttime.
- Regression model showed significant limitation in terms of timing and intensity of O.T.

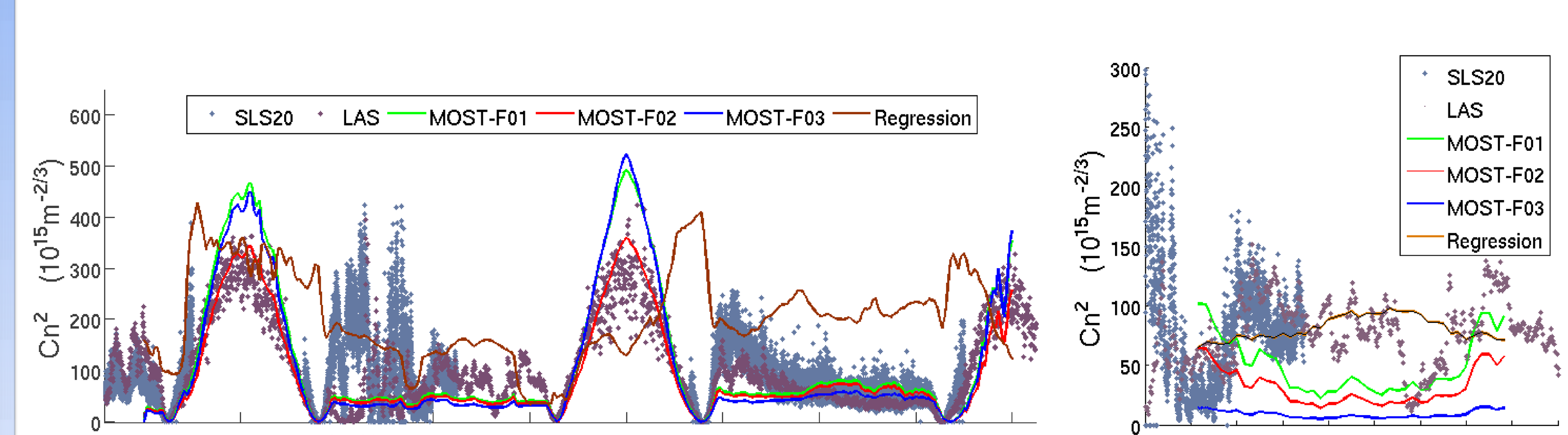

Fig. 10 Time series of C_n^2 simulated by WRF (left) and LES (right).

Future Work

- C_T^2 will be calculated directly from the temperature structure function using LES –generated flow fields output:

$$< [T(x+r) - T(x)]^2 >= C_T^2 r^{2/3}$$

- Optical turbulence data from a coastal site will be analyzed and simulated (field experiment at Beaufort, NC currently ongoing).
- New MOST function will be developed from the LES and observational databases.

Selected References

Basu, Sukanta, and Fernando Porté-Agel. "Large-eddy simulation of stably stratified atmospheric boundary layer turbulence: a scale-dependent dynamic modeling approach." *arXiv preprint physics/0502134* (2005).

Burger, Liesl, Igor A. Litvin, and Andrew Forbes. "Simulating atmospheric turbulence using a phase-only spatial light modulator." *South African Journal of Science* 104.3-4 (2008): 129-134.

Cheinet, S., et al. "The use of weather forecasts to characterize near-surface optical turbulence." *BLM* 138.3 (2011): 453-473.

Hartogensis, Oscar. *Exploring scintillometry in the stable atmospheric surface layer*. Wageningen Universiteit, 2006.

Hutt et al. "Modeling and measurements of atmospheric optical turbulence over land." *Optical Engineering* 38.8 (1999): 1288-1295.

Liu, Yubao, et al. "Simultaneous nested modeling from the synoptic scale to the LES scale for wind energy applications." *Journal of Wind Engineering and Industrial Aerodynamics* 99.4 (2011): 308-319.

Sadot, Dan, and Norman S. Kopeika. "Forecasting optical turbulence strength on the basis of macroscale meteorology and aerosols: models and validation." *Optical Engineering* 31.2 (1992): 200-212.

Wang, Yao and Basu, Sukanta (2013), Realistic Stable Boundary Layer Turbulence Generation: A Coupled Mesoscale-Large-Eddy Modeling Framework. (under preparing)

Tatarskii, Valerian Ilich. "Wave propagation in turbulent medium." *Wave Propagation in Turbulent Medium, by Valerian Ilich Tatarskii. Translated by RA Silverman. 285pp. Published by McGraw-Hill, 1961.* 1 (1961).